# Avoiding ventilator-associated pneumonia: Curcumin-functionalized endotracheal tube and photodynamic action

Amanda C. Zangirolami[a], Lucas D. Dias[a], Kate C. Blanco[a], Carolina S. Vinagreiro[b], Natalia M. Inada[a], Luis G. Arnaut[b], Mariette M. Pereira[b], and Vanderlei S. Bagnato[a,c,1]

[a]São Carlos Institute of Physics, University of São Paulo, São Carlos, SP 13566-590, Brazil; [b]Coimbra Chemistry Centre, Department of Chemistry, University of Coimbra, 3004-535 Coimbra, Portugal; and [c]The Hagler Institute for Advanced Studies, Texas A&M University, College Station, TX 77843-3120

Contributed by Vanderlei S. Bagnato, July 10, 2020 (sent for review April 16, 2020; reviewed by Merrill A. Biel and Tayyaba Hasan)

**Hospital-acquired infections are a global health problem that threatens patients' treatment in intensive care units, causing thousands of deaths and a considerable increase in hospitalization costs. The endotracheal tube (ETT) is a medical device placed in the patient's trachea to assist breathing and delivering oxygen into the lungs. However, bacterial biofilms forming at the surface of the ETT and the development of multidrug-resistant bacteria are considered the primary causes of ventilator-associated pneumonia (VAP), a severe hospital-acquired infection for significant mortality. Under these circumstances, there has been a need to administrate antibiotics together. Although necessary, it has led to a rapid increase in bacterial resistance to antibiotics. Therefore, it becomes necessary to develop alternatives to prevent and combat these bacterial infections. One possibility is to turn the ETT itself into a bactericide. Some examples reported in the literature present drawbacks. To overcome those issues, we have designed a photosensitizer-containing ETT to be used in photodynamic inactivation (PDI) to avoid bacteria biofilm formation and prevent VAP occurrence during tracheal intubation. This work describes ETT's functionalization with curcumin photosensitizer, as well as its evaluation in PDI against *Staphylococcus aureus*, *Pseudomonas aeruginosa*, and *Escherichia coli*. A significant photoinactivation (up to 95%) against Gram-negative and Gram-positive bacteria was observed when curcumin-functionalized endotracheal (ETT-curc) was used. These remarkable results demonstrate this strategy's potential to combat hospital-acquired infections and contribute to fighting antimicrobial resistance.**

hospital-acquired infection | ventilator-associated pneumonia | biofilms | endotracheal tube | photodynamic therapy

Hospital-acquired infections are a worldwide public health problem, causing thousands of deaths every day (1) in addition to increased healthcare costs (the United States: $33 billion per year, ref. 2; Europe: €13–24 billion per year, ref. 3). Among hospital procedures, mechanical ventilation with an endotracheal tube (ETT) is commonly used to facilitate the oxygen flow from the oropharynx into the trachea (4) in postoperative or posttraumatic patients. However, its use may increase the risk of nosocomial pneumonia by 6–21 times (5, 6). These occur since bacteria from the environment aggregate on the ETT surface. Therefore, they become permanently attached and can later be broncho-aspirated. This colonization produces extracellular polysaccharides and develops a microbial biofilm and, in most of these cases, leads to ventilator-associated pneumonia (VAP) (7–9). The infection is hard to fight since colonies are formed in the airways, where the adaptation mechanisms include changes in quorum sensing and the consequent production of virulence factors. Thus, oral or systemic antibiotics have shown intrinsic difficulties in acting, and the problem becomes even more severe when bacteria develop additional resistance.

In this regard, the use of an antimicrobial-coated ETT is currently a vital strategy to reduce and eliminate biofilm formation and, hence, VAP (10, 11). Different coatings on the ETT have been used to reach this aim, such as silver sulfadiazine (12), silver (13–16), silver sulfadiazine/chlorhexidine (17), gentamicin (18), silver-palladium-gold (19), rose bengal (11), and gendine (10). Most of them present some antibacterial effect but present limitations as well (12).

Besides coating with metals or metal-based particles, other studies have demonstrated that photodynamic therapy (PDT) is a useful tool on microorganism photoinactivation and can become a potential alternative for the treatment and eradication of microbial infections (20–27). PDT combines an appropriate source light, a photosensitizer, and molecular oxygen ($O_2$) to produce reactive oxygen species (ROS: singlet oxygen and oxygen-centered radicals), destroying targeted cells and microorganisms (28–31). Furthermore, PDT is simple to use and can be repeated. It offers a long-term treatment to obtain complete elimination of biofilms, a cost-effective therapeutic option, and an independent approach toward the resistance pattern of bacteria to antibiotics, showing the absence of photoresistant strains (32–36). According to recent literature (37), the infectious focus is in the region of contact, as shown in Fig. 1, which is the region where the microorganisms can migrate to the lungs, resulting in

## Significance

Hospital-acquired infections also caused by multidrug-resistant bacteria are currently one of the most severe problems that our society faces, which constitute an excellent risk for humankind. The absence of alternatives to combat these types of infections leaves humanity highly vulnerable. Therefore, it becomes imperative to develop new technologies to fight bacterial infections, with alternative mechanisms of action relative to the classical antibiotics. Since ventilator-associated pneumonia (VAP) occurs in patients under mechanical ventilation, an urgent need is needed to prevent, decrease, and combat infectious pathogens at the endotracheal tube (ETT). In this paper, we demonstrate a practical methodology to prepare a regular photosensitizer-containing ETT, with effective photodynamic activity for microbial inactivation. The process is efficient and safe for the patient.

Author contributions: K.C.B., M.M.P., and V.S.B. designed research; A.C.Z., L.D.D., K.C.B., C.S.V., and N.M.I. performed research; L.D.D., L.G.A., and M.M.P. contributed new analytic tools; A.C.Z., L.D.D., K.C.B., M.M.P., and V.S.B. analyzed data; and A.C.Z., L.D.D., K.C.B., M.M.P., and V.S.B. wrote the paper.

Reviewers: M.A.B., University of Minnesota Medical Center; and T.H., Harvard Medical School.

The authors declare no competing interest.



[1]To whom correspondence may be addressed. Email: vander@ifsc.usp.br.

This article contains supporting information online at https://www.pnas.org/lookup/suppl/doi:10.1073/pnas.2006759117/-/DCSupplemental.

First published August 31, 2020.

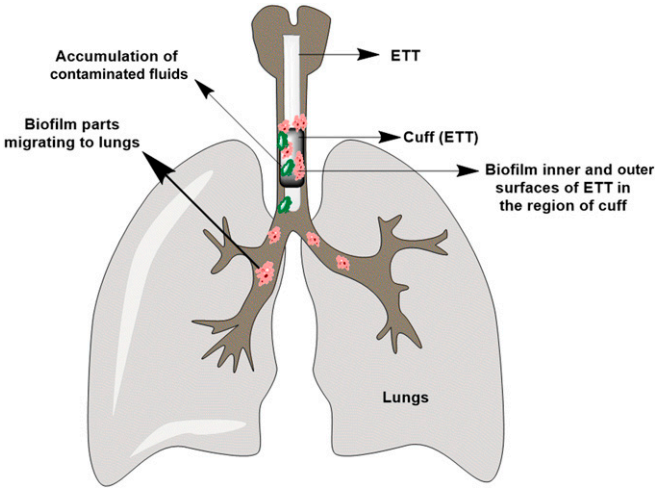


**Fig. 1.** Representative diagram of ETT positioning. Contact is made by the cuff located at the lower end, allowing the action of the breathing machine. At this point lies the critical part of accumulation of contaminated liquids and the formation of biofilms that lead to infections.

VAP. It is necessary to go much further, by promoting inactivation mainly in the region of the inflated balloon contact and beyond. Similarly, bathing the tube and promoting lighting does not help much, due to leaching of the fluids that wash out the photosensitizer from the interest region. The tube itself must be a photosensitizer. Among photosensitizers used so far, curcumin is one of the most studied molecules with high antimicrobial activity (38–40), showing three reactive functional groups (one diketone moiety and two phenolic groups) (41). The curcumin antibacterial effects are related to ROS production and intracellular accumulation, causing irreversible bacterial cell membrane damage, leading to cell death even in biofilms form (42).

Based on this knowledge, the aim of this study is focused on the development of an efficient chemically bonded photosensitizer to the ETT, introduced in the airway, promoting PDT with reduction/elimination of biofilm formation in orotracheal intubation to prevent the lungs from infections, overcoming presently posed limitations. Here, we report the chemical functionalization of commercially available polyvinyl chloride (PVC)-based ETT with curcumin photosensitizer and demonstrate the potentialities of its practical use. Spectroscopic and mechanical characterization of the curcumin-functionalized endotracheal tube (ETT-curc) has shown the maintenance of its required properties and allowed to investigate the mechanism of action of microorganism's inactivation at the ETT surface. Antimicrobial activity and biofilm inhibition by the ETT-curc were evaluated against Gram-negative bacteria (*Pseudomonas aeruginosa* and *Escherichia coli*) and Gram-positive bacteria (*Staphylococcus aureus*). Finally, this functionalization is performed with an entirely safe and innocuous substance that does not provide any significant modification of the ETT properties, and the presence of the organism does not constitute any risk for the patients.

## Results

**Preparation of Curcumin-PVC–Based Endotracheal Tube.** The ETT system is in permanent contact with the air track's liquids. Considering that biofilms formed both on the outside and inside the tube, the polymer surface's chemical functionalization with photosensitizing molecules constitutes the best approach for the preparation of photoactivated ETT, as shown in Fig. 2. Moreover, this approach prevents the continuous washing of the photosensitizer, which is a crucial issue for its long-living action.

This study started with the linkage of the curcumin photosensitizer onto clinically approved ETT (Fig. 3*A*) made by PVC. First, the chemical stability was evaluated in different organic solvents at several temperatures. For that, the ETT was divided into small fragments, which were introduced in a different flask containing organic solvents, such as 1,2-dimethoxyethane (DME), dichloromethane (DCM), ethyl acetate (EtOAc), tetrahydrofuran (THF), and dimethyl sulfoxide (DMSO) within a temperature ranging from 30 °C to 50 °C (*SI Appendix*, Table S1). Then, optimization studies, at a small scale, were performed to promote the covalent linkage of curcumin to PVC-based ETT. From the macroscopic structural analysis of the ETT, it was concluded that the most efficient approach was the one that used DMSO as solvent and $Cs_2CO_3$ base, an under inert atmosphere, along 4 h (Fig. 2). The final solution's ultraviolet-visible (UV-Vis) measurements determined the indirect quantification of the amount of functionalized curcumin compared with a standard 0.5% curcumin solution. A homemade reactor was developed (*SI Appendix*, Fig. S1) to carry out the functionalization of PVC-based ETT with curcumin. The images of the clinically available ETT and the ETT-curc are presented in Fig. 3 *A* and *B*, respectively.

**Characterization of ETT-curc.** ETT-curc was characterized by UV-Vis fluorescence emission spectroscopy. The fluorescence emission spectrum, acquired from the outside surface of the ETT-curc and presented in Fig. 4, showed the steady emission band at 550 nm, typical of curcumin photosensitizer.

FT-IR spectroscopy was then used to characterize the small pieces of the ETT-curc compared with curcumin and non-functionalized ETT material (*SI Appendix*, Figs. S2 and S5). The FT-IR spectrum of curcumin showed characteristic vibrational peaks at 3,509 $cm^{-1}$ (hydroxyl group -OH), 1,600–1,650 $cm^{-1}$ (C = O), 1,509 $cm^{-1}$ (C = C ethylene), and 1,250 $cm^{-1}$ (C-O-C group ether). The spectrum of ETT-curc presented similar peaks at 3,506 $cm^{-1}$ (hydroxyl group -OH), 1,600–1,650 $cm^{-1}$ (C = O), 1,512 $cm^{-1}$ (C = C ethylene), and 3,432 $cm^{-1}$ (water), which corroborated with the presence of curcumin on ETT-curc. The saddle shift between the pure curcumin spectrum with the ETT-curc indicates the molecules' chemical bond to the polymer surface. Moreover, the shift and shape modification on the OH group vibration (3,510 $cm^{-1}$) and the C = O vibration (1,628 $cm^{-1}$) are indicative of the chemical bond between curcumin photosensitizer and the polymer surface (43).

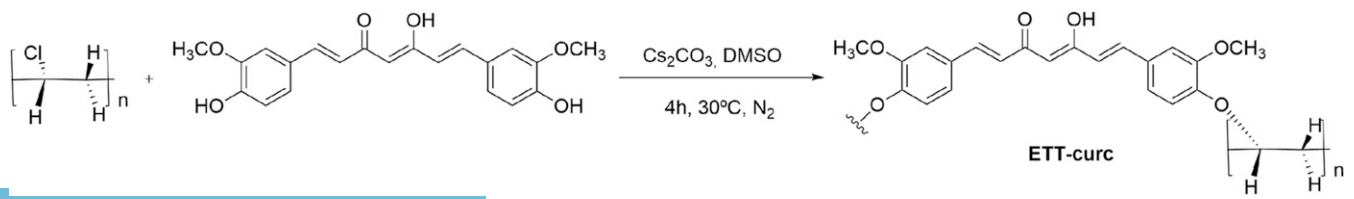


**Fig. 2.** Scheme of the covalent linkage of curcumin photosensitizer onto PVC-based ETT.

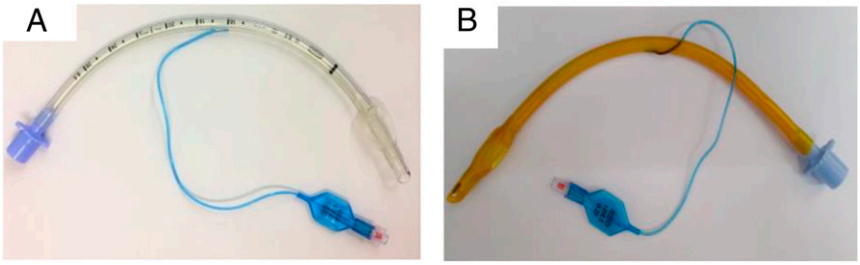


**Fig. 3.** (*A*) PVC-based ETT. (*B*) ETT-curc. The yellowish color of the surface indicates the presence of curcumin.

To analyze the physical structure of the ETT-curc and evaluate the efficiency of the ETT surface covering with the curcumin, scanning electron microscopy (SEM) was performed before and after the functionalization process on the ETT-curc surface (Fig. 5 *A* and *B*), respectively. As expected, the microscopy image of the nonfunctionalized ETT (Fig. 5*A*) is similar to those previously reported in the literature (44). In contrast, ETT-curc clearly shows the presence of the curcumin photosensitizer on the ETT surface without altering its global physical structure (Fig. 5*B*). It should be noted that preserving the original tube's quality is of fundamental importance for an application. Moreover, the presence of curcumin in the ETT-curc whole area guarantees that no biofilm misses the action of the photoactivated curcumin. That is an essential characteristic to guarantee the efficiency of microorganism's elimination on ETT.-6354777740000 Besides, both ETT and ETT-curc were submitted to tensile tests to evaluate the mechanical properties maintenance after the functionalization procedure (*SI Appendix*, Fig. S3). Each tube was subjected to a force (axial direction of the ETT) that tended to move them to rupture. Fig. 6 shows the tensile stress (MPa) vs. tensile strain (%) of ETT (black) and ETT-curc (red). Two ETT and three ETT-curc were analyzed, and the obtained values of the tensile strain 285 and 286 for ETT and 231, 236, and 263 for ETT-curc can be considered as not compromising the mechanical properties of the ETT.

The quantification of functionalized-curcumin onto ETT was calculated by UV-Vis, following the Beer–Lambert law, where the absorbance values of the initial and final reaction medium and washing solutions were measured. The difference in initial concentration and final concentration plus the washing solutions gave a calculated percentage of 0.5% of linked curcumin. Finally, the stability of the ETT-curc, under a range of pH values (2.0, 4.5, 7.0, 8.0, and 10.0), mimicking the biological systems, was analyzed by UV-Vis absorption spectroscopy, recorded at different times (0 h, 6 h, 12 h, 24 h, 48 h, 168 h, 408 h, and 576 h), and data are presented in *SI Appendix*, Fig. S4. From the analysis of the UV-Vis spectra, it was concluded in this range of pH, the presence of curcumin or degradation products in solution was not observed in any case simulating situations corresponding to pulmonary acidosis and alkalosis.

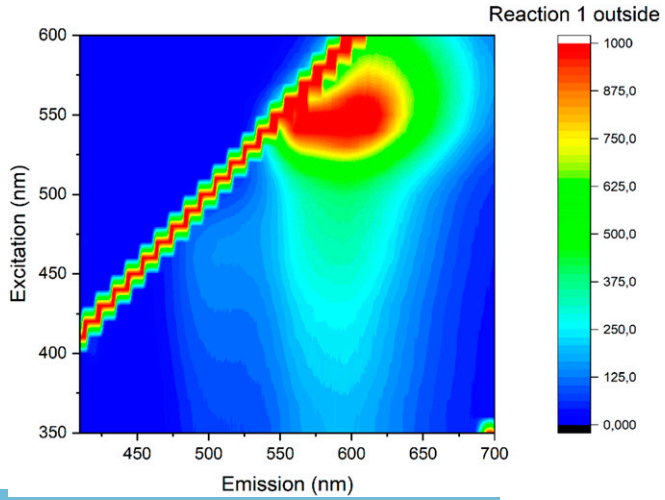


**Fig. 4.** Fluorescence spectrum on the outside surface of the ETT-curc.

**In Vitro Antimicrobial Activity Tests.** To evaluate the potential antimicrobial of the ETT-curc, in vitro tests were performed using different bacterial strains (*S. aureus*, *E. coli*, *and P. aeruginosa*) in the inner and outer surfaces of small pieces of ETT and ETT-curc. After contamination, each set of 1-cm pieces was subdivided into two groups: the first group was placed in the dark and the second group was irradiated inside and outside with 450-nm light (70 mW/cm$^2$), and a fluence rate of 50 J/cm$^2$ (illumination for 12 min). After illumination, the number of microorganisms remained in the tube was evaluated. The resulted data are presented in Fig. 7. When compared to the original ETT, all conditions led to a significant decrease in bacterial colonies. PDT action represented by the ETT-curc with light showed a significant microbial reduction, demonstrating the proof of principle proposed. The question concerning the fact that the functionalized surface has an equivalent effect as the free molecules in contact with microorganisms was confirmed. The functionalized surface promotes photodynamic action for microbial control at an acceptable level. The results indicate a single application of light, a microbial reduction of about 95% for *S. aureus*, 72% for *E. coli*, and 73% for *P. aeruginosa*, compared with the control. The PDT groups are statically different from the control groups ($P < 0.05$). Such a reduction, with a single illumination, is a quite promising result, which might be even better if the illumination is repeated. In a second in vitro experiment, the continuous growth of the biofilm after illumination was simulated. Considering that the ETT installed in patients is in constant exposure to bacterial species and an ideal nutritional and environmental conditions for pathogenic strains development is present, an in vitro simulation of this scenario, together with the treatment proposed in this study, was performed. The results are presented in Fig. 8. The ETT-curc containing bacterial biofilm (*S. aureus*) was irradiated, at 50 J/cm$^2$, (once every 24 h) and evaluated along 6 d. After each illumination, ETT-curc returned to optimal microbial growth conditions. In Fig. 8, it is shown that PDT reduced the number of bacterial colonies present in ETT-curc after each therapy session, although ETT-curc continues in this microbial multiplication environment. It was also shown that ETT-curc remains active after six PDT sessions with 23.76% microbial reduction. The PDT groups of days 1, 2, and 5 are statically different from the control groups. This simulation system allowed us to evaluate the possibility of implementing repeated or continuous

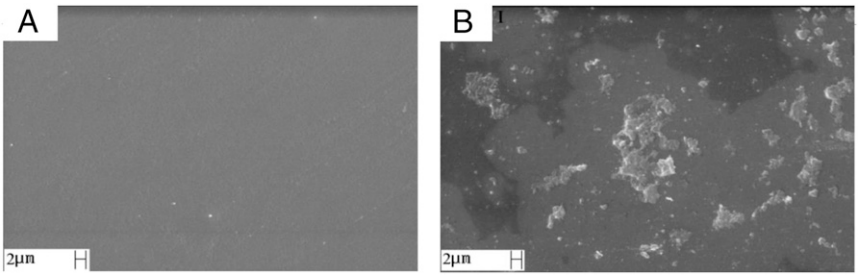


**Fig. 5.** SEM of ETT (*A*) and ETT-curc (*B*). The sample with curcumin shows good covering of the surface.

illumination without degradation of the photosensitizer immobilized onto ETT. Besides the fluctuations, the ETT-curc, without illumination, shows a prevalence of 85% (average) of the biofilm along the days when compared with control (ETT alone). The functionalized surface without light has a small effect on the growth, consistent with a day experiment. However, the use of the ETT-curc, with illumination, provided around 40% of the control, demonstrating a considerable reduction in biofilm formation.

**Bacterial Biofilm Formation.** The experiment was designed to evaluate the biofilm's kinetics developed on the ETT without and with curcumin over time. The bacterial biofilm developed in ETT and ETT-curc in different times. After the contamination, the light groups were washed twice with a phosphate-buffered saline (PBS) solution and submitted to PDT with the Biotable device. Each experiment had three repetitions, and the groups were: 1) only bacteria on the ETT, and 2) bacteria with PS functionalized on ETT. The methodology is described in *SI Appendix*, Fig. S6. The light doses each group received are described at *SI Appendix*, Table S2.

**Fiber Illumination on ETT-curc.** In *SI Appendix*, Fig. S7, we show the way that ETT-curc is illuminated via a cylindrical diffuser fiber, placed inside the tube. To demonstrate that the minimum antimicrobial threshold dose is reached inside and outside the ETT-curc, diffused light intensities from inner-out were measured (*SI Appendix*, Fig. S8).

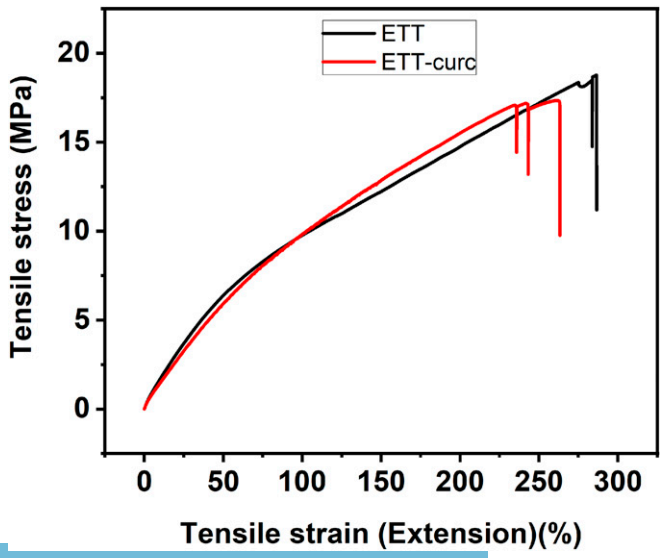


**Fig. 6.** Stress-strain curves for PVC-based ETT (black) and ETT-curc (red).

## Discussion

The main goal of this work was to functionalize a clinically approved ETT with a curcumin photosensitizer. We deliberately avoided changing EETs to make them more amenable to surface functionalization. The procedure developed can be applied to existing ETTs made of PVC. The light can penetrate the microbial biofilm considering its thickness, and the PVC does not absorb at 450 nm. We first address the reaction conditions to optimize the functionalization process regarding the solvent used, temperature, and reaction time.

The nucleophilic substitution reaction of the PVC-chlorine atom by the hydroxyl group of curcumin was strongly dependent on the reaction conditions: solvent, base, temperature, and reaction time. All of the other tested reaction conditions led to a significant physical variation of the ETT that was attributed to the removal of the plasticizers and ink dyes. The solid $Cs_2CO_3$ revealed to be the most appropriate and easily removed inorganic base, capable of generating the curcumin anion nucleophile necessary to promote the chlorine atom substitution reaction to generate the desired covalently linked curcumin to the ETT tube.

Different types of antimicrobials coatings on endotracheal tube surface to avoid VAP have been reported, e.g., gendine (10), silver sulfadiazine (12), silver (13–16), silver sulfadiazine/chlorhexidine (17), gentamicin (18), silver-palladium-gold (19), rose Bengal (11), and methylene blue. Most of them presented some antibacterial effect, but showed limitations such as: 1) lack of detailed and precise toxicity information of silver for human treatment; 2) risk of accumulation of silver in the body leading to heavy metal toxicity; 3) possibility of bacteria resistance formation along the time; 4) some results reported with silver as coating did not show decrease of bacterial colonization when compared to commercial ETT (silver free). Gendine (a combination of chlorhexidine and gentian violet) was applied as an antimicrobial coating (10), but the authors did not present any physical and chemical characterization, leaching, and stability evaluation. Regarding the PDT systems used, studies reported the application of rose Bengal (11) and methylene blue as photosensitizers. When methylene blue was reported, the authors described a different PDT protocol compared to us since they delivered the photosensitizer by spray into the lumen of the ETT, which may occur leaching. A bacterial photoinactivation was observed for the study that rose Bengal was applied (11), but a lack of experimental details (light dose used, physical and chemical characterization, coating procedure) was also observed.

Herein, we described a stable functionalization of a commercial PVC-based endotracheal tube with curcumin, a natural and nontoxic photosensitizer. From the analysis of Fig. 7, we can conclude that the ETT-curc having the surface modified with covalently linked curcumin, under dark conditions, clearly decrease the bacterial adhesion and biofilm formation on surface ETT. These results are in agreement with the literature (45), where it has been demonstrated that biofilm architectures

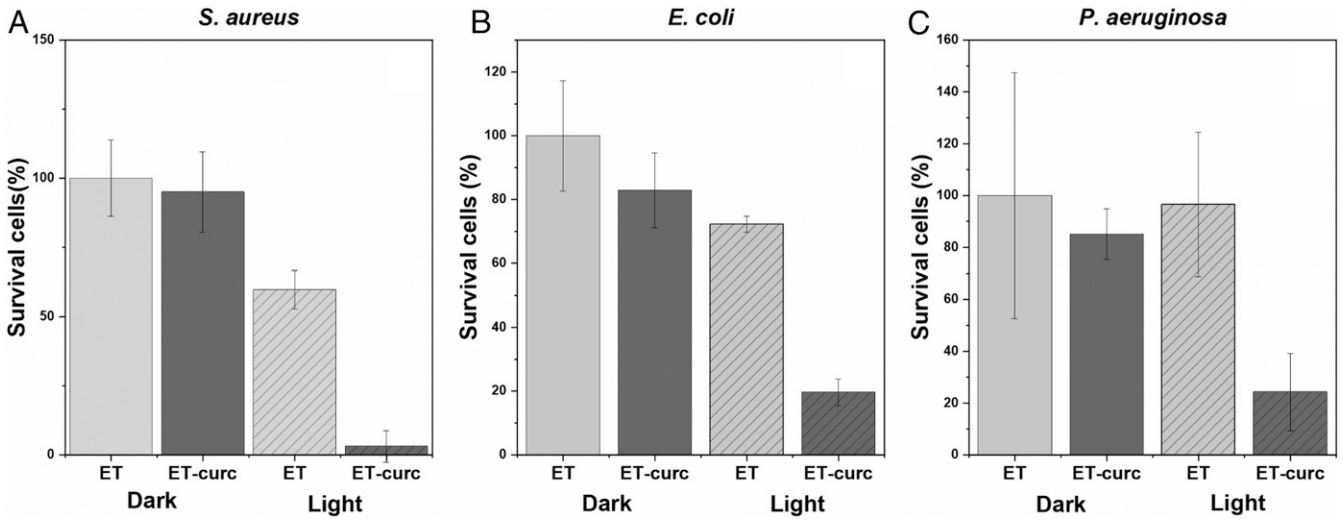


**Fig. 7.** Photodynamic inactivation of bacterial species *S. aureus* (*A*), *E. coli* (*B*) and *P. aeruginosa* (*C*) in biofilms contained in ETT and ETT-curc, before and after being submitted to total light dose of 50 J/cm$^2$ ($n$ = 9, error bar = SD and $P < 0.05$).

determine the relative strength of the mechanical cell-cell attraction and repulsion forces. In this study, the presence of curcumin photosensitizer attached to the ETT may produce an alteration in the mechanical cell-cell forces, with consequent modifications and reduction of biofilm formation.

These results point out that typical ROS formation by curcumin in the planktonic medium is also observed in this *S. aureus* bacteria biofilm destruction, using the ETT-curc device. Based on these results, we conclude that electrostatic repulsions between photosensitizer molecules and the biofilm polysaccharides structure might contribute to biofilm restructuring and cell death. Furthermore, based on these results, we hypothesize that biofilm architectures are primarily determined by the relative strength of the active mechanical cell-cell attraction and repulsion forces. To apply this principle in clinical cases, a balance between the rate of biofilm formation versus the rate of bacterial inactivation by PDT action should be considered. The data obtained in this work provide an essential tool to rationalize the ideal conditions for the optimization of such balance. If we imagine that the inhibition rate by constant illumination exceeds the biofilm formation rate, it is possible that the system does not accumulate colonies and have no chance of deleterious biofilm formation. However, when no lighting is used, that balance will be destroyed, allowing the film's growth to surpass the rate of destruction (Fig. 9).

This type of bio-based material may have many applications in the future. We demonstrate that the nucleophilic substitution of chlorine functionalized PVC with curcumin is an efficient approach to prepare photosensitizer-functionalized endotracheal tubes. The curcumin-functionalized endotracheal tube characterization by infrared spectroscopy, fluorescence spectroscopy, SEM, and tensile tests corroborated the effective functionalization of the curcumin onto the PVC-based endotracheal tube.

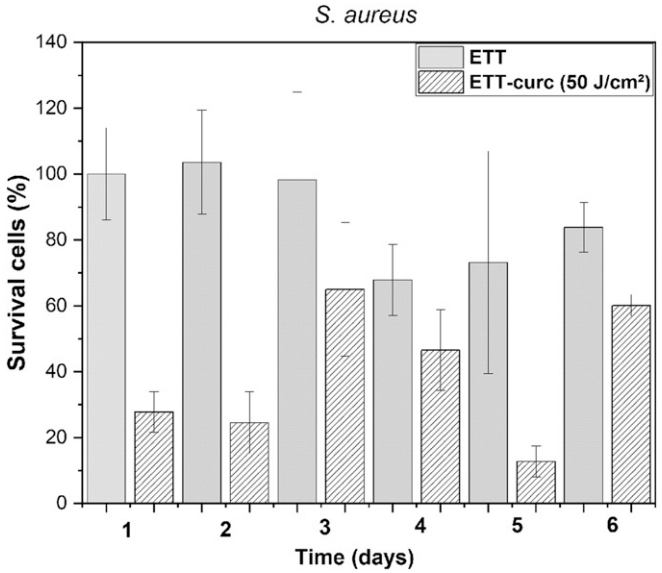


**Fig. 8.** Evaluation of PDT sessions along 6 d for ETT (solid columns) and ETT-curc (diagonally striped columns). The total light dose of each group is 50 J/cm$^2$ multiplying by the number of days ($n$ = 9, error bar = SD and $P < 0.05$).

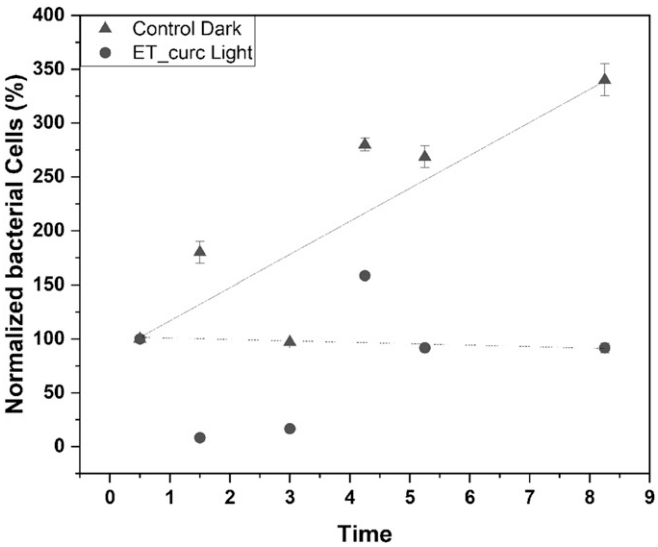


**Fig. 9.** Number of cells in the ETT and ETT-curc groups illuminated over time. The lines are merely visual references to observe the tendency of the points ($n$ = 7, error bar = SD and $P < 0.05$).

ETT-curc shows a robust photodynamic inactivation under blue light activation (at 450 nm) against *E. coli* (72%), *S. aureus* (95%), and *P. aeruginosa* (73%). Furthermore, no degradation and leaching were observed for curcumin-functionalized endotracheal tube under a range of pH (2.0, 4.5, 7.0, 8.0, and 10.0). The findings described herein allow us to foresee the significance of this type of photosensitizer-functionalized materials in many applications. It can significantly reduce the number of deaths from hospital-acquired infections caused by multidrug-resistant bacteria.

## Materials and Methods

**Preparation of ETT-curc.** A handmade reactor (*SI Appendix*, Fig. S1), with an appropriate size, was designed to perform the complete ETT homogeneous functionalization. The ETT was placed inside the reactor, and several cycles of vacuum/$N_2$ gas were performed. Curcumin (4.95 mg/mL) and $Cs_2CO_3$ (24.8 mg/mL) solution was introduced into the reactor via cannula, for 4 h, at 30 °C, under an inert atmosphere after the tube was washed and tested (*SI Appendix, Experimental Procedures*).

**Biofilm Photodynamic Inactivation.** In vitro tests with inhibition of biofilm formation of the functionalized ETT-curc in absence and presence of illumination were performed using the ETT as a control experiment. A preinoculum of *S. aureus*, *E. coli*, and *P. aeruginosa* strains was prepared with brain heart infusion (BHI) along 15 h. After this period, the bacterial cells were washed twice with phosphate buffer, and 100 μL of each inoculum solution was added to a 24-well plate containing 900 μL of BHI medium and pieces (1 cm) of the ETT and ETT-curc. To allow the bacterial biofilm formation around the ETT, they were incubated for 24 h at 37 °C. After removing the planktonic cells by washing all of the ETT with PBS, the ETT was separated into four groups. First, the biofilms formed in the surface of the control (ETT) and functionalized ETT-curc without illumination were removed with PBS from the ETT surface via mechanical stirring. Then, each solution diluted with PBS and the colony formation unity method performed, and the corresponding colony number in Fig. 7 for *S. aureus*, *E. coli*, and *P. aeruginosa*. The groups' control ETT and functionalized ETT-curc were irradiated inside and outside, with 450-nm light-emitting diode light under a total light dose of 50–350 J/cm$^2$ on each side (*SI Appendix*, Table S2). After the illumination, the biofilms were removed using PBS from the ETT surface under conditions described above, and each solution was diluted again with PBS, and the corresponding colony number presented in Fig. 7 with controls and tests presented in orange and red, respectively. Bacterial biofilm formation and statistical analysis details are presented in *SI Appendix, Experimental Procedures*.

**Data Availability.** All study data are included in the article and *SI Appendix*.

**ACKNOWLEDGMENTS.** This work was funded by Fundação de Amparo à Pesquisa do Estado de São Paulo (FAPESP) Grant CEPOF 2013/07276-1, INCT "*Basic Optics and Applied to Life Sciences*" Grant FAPESP 2014/50857-8, Conselho Nacional de Desenvolvimento Científico e Tecnológico (CNPq) Grant 465360/2014-9, Fundação para a Ciência e a Tecnologia (FCT), and QREN/FEDER Grants UID/QUI/00313/2019 and POCI-01-0145-FEDER-027996. We thank FAPESP, Coordenação de Aperfeiçoamento de Pessoal de Nível Superior, CNPq, and FCT for scholarships namely CNPq (to A.C.Z.), FAPESP 2019/13569-8 (to L.D.D.), FAPESP 2019/12694-3 (to K.C.B.), and FCT PD/BD/128317/2017 (to C.S.V.).

1. A. W. Friedrich, Control of hospital acquired infections and antimicrobial resistance in Europe: The way to go. *Wien. Med. Wochenschr.* **169** (suppl. 1), 25–30 (2019).
2. J. A. Al-Tawfiq, P. A. Tambyah, Healthcare associated infections (HAI) perspectives. *J. Infect. Public Health* **7**, 339–344 (2014).
3. H. Arefian *et al*., Estimating extra length of stay due to healthcare-associated infections before and after implementation of a hospital-wide infection control program. *PLoS One* **14**, e0217159 (2019).
4. F. Barbier, A. Andremont, M. Wolff, L. Bouadma, Hospital-acquired pneumonia and ventilator-associated pneumonia: Recent advances in epidemiology and management. *Curr. Opin. Pulm. Med.* **19**, 216–228 (2013).
5. M. Cavalcanti *et al*., Risk and prognostic factors of ventilator-associated pneumonia in trauma patients. *Crit. Care Med.* **34**, 1067–1072 (2006).
6. R. Pinciroli, C. Mietto, L. Berra, Respiratory therapy device modifications to prevent ventilator-associated pneumonia. *Curr. Opin. Infect. Dis.* **26**, 175–183 (2013).
7. C. Sarda, F. Fazal, J. Rello, Management of ventilator-associated pneumonia (VAP) caused by resistant gram-negative bacteria: Which is the best strategy to treat? *Expert Rev. Respir. Med.* **13**, 787–798 (2019).
8. X. Xie, J. Lyu, T. Hussain, M. Li, Drug prevention and control of ventilator-associated Pneumonia. *Front. Pharmacol.* **10**, 298 (2019).
9. L. A. Mandell, M. S. Niederman, Aspiration Pneumonia. *N. Engl. J. Med.* **380**, 651–663 (2019).
10. G. Chaiban, H. Hanna, T. Dvorak, I. Raad, A rapid method of impregnating endotracheal tubes and urinary catheters with gendine: A novel antiseptic agent. *J. Antimicrob. Chemother.* **55**, 51–56 (2005).
11. L. Berra *et al*., Antimicrobial-coated endotracheal tubes: An experimental study. *Intensive Care Med.* **34**, 1020–1029 (2008).
12. L. Berra *et al*., Internally coated endotracheal tubes with silver sulfadiazine in polyurethane to prevent bacterial colonization: A clinical trial. *Intensive Care Med.* **34**, 1030–1037 (2008).
13. J. Rello *et al*., Reduced burden of bacterial airway colonization with a novel silver-coated endotracheal tube in a randomized multiple-center feasibility study. *Crit. Care Med.* **34**, 2766–2772 (2006).
14. P. Kalfon *et al*., Comparison of silver-impregnated with standard multi-lumen central venous catheters in critically ill patients. *Crit. Care Med.* **35**, 1032–1039 (2007).
15. L. Berra *et al*., Antibacterial-coated tracheal tubes cleaned with the Mucus Shaver : A novel method to retain long-term bactericidal activity of coated tracheal tubes. *Intensive Care Med.* **32**, 888–893 (2006).
16. M. H. Kollef *et al*.; NASCENT Investigation Group, Silver-coated endotracheal tubes and incidence of ventilator-associated pneumonia: The NASCENT randomized trial. *J. Am. Med. Assoc.* **300**, 805–813 (2008).
17. L. Berra *et al*., Endotracheal tubes coated with antiseptics decrease bacterial colonization of the ventilator circuits, lungs, and endotracheal tube. *Anesthesiology* **100**, 1446–1456 (2004).
18. C. G. Adair *et al*., Eradication of endotracheal tube biofilm by nebulised gentamicin. *Intensive Care Med.* **28**, 426–431 (2002).
19. G. Björling *et al*., Tolerability and performance of BIP endotracheal tubes with noble metal alloy coating–A randomized clinical evaluation study. *BMC Anesthesiol.* **15**, 174–184 (2015).
20. G. Sivieri-Araujo *et al*., Rat tissue reaction and cytokine production induced by antimicrobial photodynamic therapy. *Photodiagn. Photodyn. Ther.* **18**, 315–318 (2017).
21. E. T. Carrera *et al*., The application of antimicrobial photodynamic therapy (aPDT) in dentistry: A critical review. *Laser Phys.* **26**, 123001–123024 (2016).
22. C. C. C. Quishida *et al*., Photodynamic inactivation of a multispecies biofilm using curcumin and LED light. *Lasers Med. Sci.* **31**, 997–1009 (2016).
23. C. C. C. Quishida *et al*., Photodynamic inactivation of a multispecies biofilm using Photodithazine(®) and LED light after one and three successive applications. *Lasers Med. Sci.* **30**, 2303–2312 (2015).
24. H. Vögeling *et al*., Synergistic effects of ultrasound and photodynamic therapy leading to biofilm eradication on polyurethane catheter surfaces modified with hypericin nanoformulations. *Mater. Sci. Eng. C* **103**, 109749 (2019).
25. J. Tan, Z. Liu, Y. Sun, L. Yang, L. Gao, Inhibitory effects of photodynamic inactivation on planktonic cells and biofilms of Candida auris. *Mycopathologia* **184**, 525–531 (2019).
26. C.-T. Chien *et al*., The antimicrobial photodynamic inactivation resistance of Candida albicans is modulated by the Hog1 pathway and the Cap1 transcription factor. *Med. Mycol.* **57**, 618–627 (2018).
27. Q. Jia, Q. Song, P. Li, W. Huang, Rejuvenated photodynamic therapy for bacterial infections. *Adv. Healthc. Mater.* **8**, e1900608 (2019).
28. Y.-Y. Wang, Y.-C. Liu, H. Sun, D.-S. Guo, Type I photodynamic therapy by organic–inorganic hybrid materials: From strategies to applications. *Coord. Chem. Rev.* **395**, 46–62 (2019).
29. L. Sobotta, P. Skupin-Mrugalska, J. Piskorz, J. Mielcarek, Porphyrinoid photosensitizers mediated photodynamic inactivation against bacteria. *Eur. J. Med. Chem.* **175**, 72–106 (2019).
30. J. M. Dąbrowski, "Chapter nine–Reactive oxygen species in photodynamic therapy: Mechanisms of their generation and potentiation" in *Advances in Inorganic Chemistry*, R. van Eldik, C. D. Hubbard, Eds. (Academic Press, 2017), Vol. vol. 70, pp. 343–394.
31. J.-O. Yoo, K.-S. Ha, "Chapter four–New insights into the mechanisms for photodynamic therapy-induced cancer cell death" in *International Review of Cell and Molecular Biology*, K. W. Jeon, Ed. (Academic Press, 2012), Vol. vol. 295, pp. 139–174.
32. G. Valduga, G. Bertoloni, E. Reddi, G. Jori, Effect of extracellularly generated singlet oxygen on gram-positive and gram-negative bacteria. *J. Photochem. Photobiol. B* **21**, 81–86 (1993).
33. A. Tavares *et al*., Antimicrobial photodynamic therapy: Study of bacterial recovery viability and potential development of resistance after treatment. *Mar. Drugs* **8**, 91–105 (2010).

34. L. Costa *et al*., Evaluation of resistance development and viability recovery by a non-enveloped virus after repeated cycles of aPDT. *Antiviral Res.* **91**, 278–282 (2011).
35. J. L. Wardlaw, T. J. Sullivan, C. N. Lux, F. W. Austin, Photodynamic therapy against common bacteria causing wound and skin infections. *Vet. J.* **192**, 374–377 (2012).
36. S. Songca, O. Oluwafemi, Photodynamic therapy: A new light for the developing world. *Afr. J. Biotechnol.* **12**, 3590–3599 (2013).
37. M. Barnes, C. Feit, T.-A. Grant, E. J. Brisbois, Antimicrobial polymer modifications to reduce microbial bioburden on endotracheal tubes and ventilator associated pneumonia. *Acta Biomater.* **91**, 220–234 (2019).
38. A. Punjataewakupt, S. Napavichayanun, P. Aramwit, The downside of antimicrobial agents for wound healing. *Eur. J. Clin. Microbiol. Infect. Dis.* **38**, 39–54 (2019).
39. A. Reshma, V. Brindha Priyadarisini, K. Amutha, Sustainable antimicrobial finishing of fabrics using natural bioactive agents- a review. *Int. J. Life Sci. Pharma Res.* **8**, 10–20 (2018).
40. C. Santezi, B. D. Reina, L. N. Dovigo, Curcumin-mediated photodynamic therapy for the treatment of oral infections-A review. *Photodiagn. Photodyn. Ther.* **21**, 409–415 (2018).
41. P. Anand, A. B. Kunnumakkara, R. A. Newman, B. B. Aggarwal, Bioavailability of curcumin: Problems and promises. *Mol. Pharm.* **4**, 807–818 (2007).
42. Y. Jiang, A. W. Leung, H. Hua, X. Rao, C. Xu, Photodynamic action of LED-activated curcumin against Staphylococcus aureus involving intracellular ROS increase and membrane damage. *Int. J. Photoenergy* **2014**, 1–8 (2014).
43. M. H. Le *et al*., The dual effect of curcumin nanoparticles encapsulated by 1-3/1-6 β-glucan from medicinal mushrooms Hericium erinaceus and Ganoderma lucidum. *Adv. Nat. Sci.: Nanosci. Nanotechnol.* **7**, 045019 (2016).
44. A. De Campos, "Blendas de PVC/PCL foto/termo e biotratadas com fungos de solo (Phanerochaete chrysosporium e Aspergillus fumigatus)," Master thesis, Universidade Estadual Paulista "Júlio de Mesquita Filho," Rio Claro, Brazil (2004).
45. R. Hartmann *et al*., Emergence of three-dimensional order and structure in growing biofilms. *Nat. Phys.* **15**, 251–256 (2019).